Article:
Ding, L., Wang, Y., Wu, P. et al. (2019) Kinematic information aided user-centric 5G vehicular networks in support of cooperative perception for automated driving. IEEE Access, 7. pp. 40195-40209. ISSN: 2169-3536

https://doi.org/10.1109/ACCESS.2019.2901985

IEEE Access
Multidisciplinary | Rapid Review | Open Access Journal

Received February 22, 2019, accepted February 24, 2019, date of publication February 27, 2019, date of current version April 9, 2019.

Digital Object Identifier 10.1109/ACCESS.2019.2901985

Kinematic Information Aided User-Centric 5G Vehicular Networks in Support of Cooperative Perception for Automated Driving

LIQIN DING[1], (Member, IEEE), YANG WANG[1], PENG WU[1], (Student Member, IEEE), LIMING LI[1], AND JILIANG ZHANG[2], (Senior Member, IEEE)

[1]School of Electronic and Information Engineering, Harbin Institute of Technology, Shenzhen 518055, China
[2]Department of Electronic and Electrical Engineering, The University of Sheffield, Sheffield S1 4ET, U.K.

Corresponding author: Yang Wang (yangw@hit.edu.cn)

This work was supported in part by the China Postdoctoral Science Foundation under Grant 2018M641829, in part by the International Science and Technology Cooperation Program of China under Grant 2017YFE0118900, and in part by the Science and Technology Project of Shenzhen under Grant JCYJ20170815140215733 and Grant JSGG20170822173002341.

ABSTRACT The cooperative perception of the driving environment via the sharing of locally sensed information among automated vehicles plays a fundamental role in ensuring the basic safety of automated driving in complicated public traffic. However, demanding requirements ranging from high data rate and large user density to ultra-high reliability and low latency, are imposed on the 5G network, which is considered the key enabler of cooperative automated driving. In this paper, we propose a novel ultra-dense 5G vehicular network architecture, which features the kinematic information aided user-centric access, to address these requirements. In particular, distributed local access and application centers (LAACs) are designed to perform application implementation and access control collectively, such that the kinematic information of the vehicles extracted at the application layer can be exploited in the dynamic management of network resources to sustain consistently high-performance wireless communications between vehicles and their serving LAACs. Focusing on the uplink transmission of the periodic cooperative sensing messages (CSMs), the possible design of key elements in the kinematic information aided user-centric access, including access point association, radio resource allocation, and mobility support, are discussed. Issues brought about by the practical network deployment and constraints are also considered. In addition, a practical benchmarking access strategy set, which addresses both the reliability and the latency requirements of CSMs, is proposed and evaluated by simulation under the freeway and intersection scenarios.

INDEX TERMS Vehicular communications, user-centric access, ultra-reliable and low-latency communications, automated driving, cooperative perception.

I. INTRODUCTION

The automotive industry is seeing two emerging technologies that may one day push a paradigm shift to the road transportation ecosystem: vehicular communications and automated driving. Vehicular communications allows vehicles to exchange useful information with each other (V2V) and with any entity that may affect their maneuvers, either a roadside infrastructure (V2I), a pedestrian (V2P), or a backend server (V2N), collectively referred to as V2X [1]. The vehicular communications standards available today, namely, the IEEE 802.11p based Dedicated Short-Range Communications (DSRC)/ETSI ITS-G5 and the cellular based LTE-V [4], are developed to support the dissemination of the state information of the vehicles (vehicle type, position, speed, acceleration, etc.) and the traffic (phases of traffic lights, road work, traffic jam, etc.) among cooperative vehicles and roadside infrastructures. The purpose is to achieve **cooperative awareness** and provide a list of driver-assistant Cooperative-Intelligent Transportation System (C-ITS) applications to improve road safety and efficiency [5], [6]. Facility layer messages such as the periodic Cooperative Awareness Messages (CAMs) and the event-driven Decentralized Environmental Notification Messages (DENMs) are standardized to

The associate editor coordinating the review of this manuscript and approving it for publication was Zhaolong Ning.

convey these state information. In general, their payload sizes are small and the associated communication requirements, in terms of data rate, end-to-end (E2E) latency, and reliability, are not very strict [5].

Automated driving, on the other hand, aims at liberating the drivers from the tiresome driving tasks and reducing human errors by deploying perception, planning and control capabilities to vehicles [2], [3]. With the rapid progress in high-performance hardwares and algorithms, the development of automated vehicles is speeding up in recent years. There already are automated passenger vehicles and commercial vehicles operating on dedicated roads under certain conditions, usually at low speed. However, their extension to complicated public traffic and high speed is fundamentally prohibited by the line-of-sight sensing range of the onboard perception systems, and their impacts on the safety and efficiency of the entire traffic might not be as positive as expected [7]–[9]. For these reasons, the integration of vehicular communications in automated driving turns out to be a must, not just an option.

The supporting role of vehicular communications to automated driving comes in different stages [10]. First and foremost, it is expected to enable **cooperative perception** for an adequate and reliable perception of the complicated driving environment, via the sharing of sensing information among automated vehicles [11]–[14]. The requirements on the underlying vehicular communications are way more demanding than those achieved by DSRC or LTE-V, and are expected to be addressed by 5G [15]–[19]. Due to the life-critical nature, vehicular communications in support of automated driving is often categorized as a typical ultra-reliable and low-latency communication (URLLC) service of 5G [20], [21]. However, it should be noted that the actual traffic patterns and communication requirements could be very different from one use case to another and vary under different scenarios [18]. In this work, we focus on cooperative perception not only because of the fundamental role it plays in automated driving, but also due to the high requirements it places simultaneously on the data rate, user density, network throughput, transmission reliability and latency, as will be explained in Section II.

The mobile network in the 5G era is undergoing revolutionary changes in both network architecture and radio access technologies [22]. Cloud computing capability is being deployed close to the radio access network (RAN) by mobile edge computing (MEC) [23]–[25]. Computationally heavy tasks can therefore be offloaded to the MEC servers from the end-devices [26]–[29]. Meanwhile, part of the core network functions is being moved to the network edge to allow local data forwarding. The ultra-dense deployment of access points (APs) is identified the key enabler to accommodate the ever increasing traffic density in 5G [30]. However, ultra-dense networks (UDNs) impose significant challenges including frequent handover and severe inter-cell interference to the current cell-centric RAN. To cope with these challenges, techniques including software defined networking (SDN) and network function virtualization (NFV) are exploited to enable the virtualization of 5G RAN and thus the user-centric access schemes [31]–[36]. In the user-centric UDN, the dense APs are formulated into logical cells and provide access service to users cooperatively. Especially, APs constituting a logical cell are renewed dynamically following the movement of the user, such that from the user's perspective, it always locates at the center of the logical cell and enjoys consistently high Quality-of-Experience (QoE). Radio resources are managed by the distributed local controllers and provided to the users in a coordinated manner. Hence, high reliability and low latency can potentially be achieved.

In cell-centric UDNs, users moving at high speed will cross the cell boundaries very often. The magnified handover rates and the large number of nearby APs will result in excessive signaling overhead. Therefore, UDNs are considered not suitable to vehicular communications until the user-centric access strategy was introduced. In [33], the channel state information (CSI) aging problem caused by high mobility was emphasized. A novel radio frame structure for CSI estimation and a spatial domain scheduler which takes CSI aging into account were proposed, and the gain they brought to the user throughput was shown. In [37], the vehicular mobility performances, in terms of the handover rate and the overhead ratio, were analyzed using stochastic geometry tools. The results show a tradeoff between capacity and handover rate. In [38], considering the typical DL broadcast traffic in vehicular networks, the user-centric access was extended such that a group of adjacent vehicles are served by a logical cell together. The authors worked on power allocation to maximize the number of served vehicle groups. Yet, many fundamental problems remain unsolved in user-centric ultra-dense vehicular networks.

We identify the following key features of the user-centric ultra-dense vehicular network that motivate our study:

- Mobility support, in particular, the dynamic management of the space-time-frequency resources following the vehicles' high-speed movements, is the greatest challenge in the implementation.
- Vehicular communications are essentially application-centric. Hence, the specific traffic pattern and communication requirements of the diverse applications must be taken into account in system design.
- The movement of the vehicles are largely predictable, which makes the information of the vehicles' kinematic states extracted at the application layer good handles for mobility support.

In this work we propose a kinematic-information aided user-centric vehicular network architecture by considering applications and communications jointly. In particular, a functional entity hosted at the MEC server, called the Local Access & Application Center (LAAC), is defined to take responsibility for both application implementation and access control. We discuss how the kinematic information of the vehicles can be exploited by the LAAC for the user-centric

access to meet the rigorous communication requirements. Issues brought about by practical network deployment and constraints are discussed as well. In addition, benchmarking strategies are presented for the periodic UL transmission of cooperative sensing messages (CSMs) to enable cooperative perception, and their performances are evaluated by simulation.

The rest of the paper is organized as follows. Section II introduces the concept and importance of cooperative perception to automated driving and summarizes the associated traffic pattern and communication requirements. Section III presents the proposed system after explaining the design consideration. Section IV discusses the possible kinematic information aided user-centric access solutions. The benchmarking strategies and the simulation results are given in Section V. Section VI concludes the paper.

II. COOPERATIVE PERCEPTION IN AUTOMATED DRIVING

The capability of performing an adequate and reliable perception on the highly dynamic driving environment is the prerequisite for an automated vehicle to maneuver safely [2], [7]. Cooperative perception, enabled by the exchange of locally sensed environmental information among automated vehicles, is the key to overcome the drawbacks of the stand-alone onboard perception system. In this section, we illustrate the concept and importance from the automated driving technique perspective and identify the traffic pattern and communication requirements to support cooperative perception.

A. CONCEPT AND IMPORTANCE

Most automated vehicles being developed today are equipped with a redundant setup of high-performance sensors, including radars, lidars, mono and stereo cameras, etc. By fusing and processing the data collected by these sensors, diverse perception tasks, such as road shape and drivable region estimation, static obstacles detection, and moving objects detection, tracking, and prediction, are performed by the perception system [2], [3]. Based on the perceptional results, a detailed model of the dynamic environment, termed the local dynamic map (LDM), is developed and used for trajectory planning, motion planning and vehicle control.

However, the stand-alone perception strategy has fundamental limitations [7], [8]. The sensing ranges of the onboard sensors are limited and constrained within line-of-sight, the measurements are noisy and easily affected by environmental conditions such as light and weather (e.g., the performance of cameras will degrade in low light or bright light conditions, and lidars cannot work well in rain and snow). These factors largely prohibit the operation of automated vehicles in complicated environments such as dense urban areas, where vehicles frequently come across intersections and the streets are surrounded by high-rise buildings. In addition, the high-definition 3D lidars most automated vehicles rely on today can cost more than the vehicles they ride on, which is a huge obstacle to commercialization.

Cooperative perception is therefore proposed to overcome these drawbacks. Automated vehicles are required to share with each other the environmental information sensed by their onboard perception systems, along with their own state information. Following [8], the facility layer messages carrying the sensed information are termed CSMs in this paper. The idea is schematically illustrated in Fig. 1: With onboard perception alone, only four vehicles are detected by the automated vehicle V1. While by fusing the CSMs and CAMs shared by the four automated/cooperative vehicles, all vehicles on this road segment are captured in the LDM.

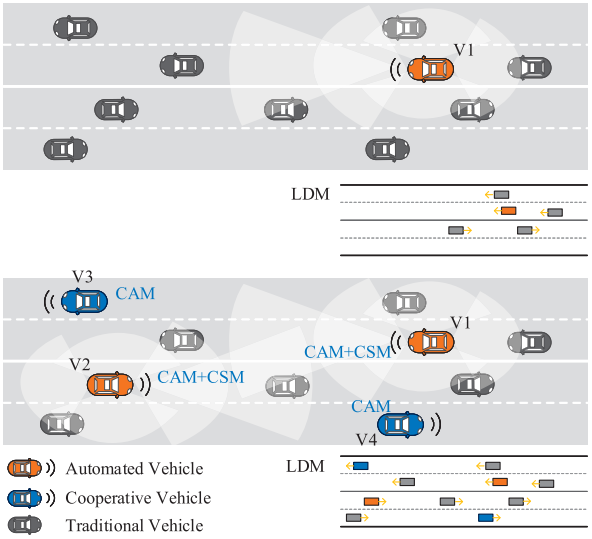

FIGURE 1. A schematic illustration of cooperative perception.

The benefits of cooperative perception are multifaceted. Firstly (and undoubtedly), the perception ranges of the automated vehicle can be extended to beyond line-of-sight and field-of-view, and thus blind spots can be eliminated. In turn, the required sensing range of an individual vehicle is reduced, making the whole system more tolerable to the sensing performance degradation caused by the unfavorable environmental conditions. Single-node-failures caused by situations like damaged or malfunctioning sensors can be largely reduced as well. Moreover, since multiple measurements of a same interested region are obtained at distributed locations and from different angles, the perception accuracy and confidence can be improved. Last but not the least, the cooperative perception strategy is more cost effective since sensors with moderate performance will satisfy and the communications devices are inexpensive in general. In practice, sensors and perception infrastructures can also be deployed at strategic spots on the road, e.g., at intersections and merge points, to further reinforce the benefits of cooperative perception.

B. TRAFFIC PATTEN AND COMMUNICATION REQUIREMENTS

Although cooperative perception has already been examined by several research bodies [8], [11]–[14], the facility layer message has not yet been standardized. Nevertheless, some consensus is achieved: To convey a comprehensive and

TABLE 1. Use cases and communication requirements.

Use case		Message payload (B)	Message rate (Hz)	E2E latency (ms)	Reliability (%)
Cooperative Awareness		50-300	≤ 10	100	90-95
Cooperative Perception	NGMN [15]	6000	≥ 10	20	99.999
	3GPP [16]	1600	10	20 3 (emergency)	99.99 99.999 (emergency)
5G URLLC [39]		32-200	/	1	99.99999

up-to-date information about the driving environment, CSMs are expected to be generated and transmitted periodically at a high frequency, and contain a detailed description of the detected objects in the environment by the onboard perception system, including main attributes such as position, heading, speed, acceleration, and the respective confidence level [8], [15], [16]. Tight E2E latency is required, since the driving environment is highly dynamic, and the information contained in the CSMs gets aged soon. Due to the life-critical nature, very high transmission reliability is demanded.

The Next Generation Mobile Networks (NGMN) Alliance estimates that the payload of a CSM could be as large as 6000 bytes, to give a detailed description of 100 detected objects. Regarding that, an E2E latency lower than 20 ms and a reliability as high as 99.999 percentage shall be guaranteed [15]. While according to the 3rd Generation Partnership Project (3GPP), the payload of a CSM should at least consist of 1600 bytes to convey the information related to 10 detected objects, and the expected E2E latency and reliability are 3ms and 99.999 percentage respectively in emergent situations, and 10ms and 99.99 percentage otherwise [16]. These requirements are much more stringent compared to those of cooperative awareness, as summarized in Table 1.

Due to the large payload sizes and strict over-the-air delay limits, high transmission rates are demanded. Besides, since cooperative perception is needed the most in dense scenarios where high vehicle density is expected, large network throughput is required to support the dissemination of the huge data volume produced by the cooperative automated vehicles per unit area. Thus, to some extent, cooperative perception covers the key features of all the three main traffic types of 5G, i.e., enhanced Mobile Broadband (eMBB), massive machine type communications (mMTC) and URLLC. Finally, the high mobility of automated vehicles brings extra challenges: the wireless channels vary rapidly in time, Doppler spreads could be large, and vehicles traverse through the cell boundaries very frequently [40]. Ensuring consistency in QoE to a large number of automated vehicles using limited radio resources is a vital problem.

III. 5G-ENABLED USER-CENTRIC VEHICULAR NETWORK ARCHITECTURE

A. DESIGN CONSIDERATIONS

It is straightforward to come up with the distributed implementation strategy for cooperative perception. Namely, each automated vehicle collects CAMs/CSMs from other vehicles located within the required perception range and develop the LDM using its onboard computer. In this regard, millimeter-wave vehicular communication technique is being considered for the short-distance sensor information exchange [41]. However, even if the messages can be delivered reliably within delay constraints, the fusing and processing of a large amount of environmental data collected by vehicles at different locations is by itself technically challenging and computationally demanding [7].

The LDM of a certain region is of the common interests to the vehicles located in it, and the CAMs/CSMs are produced and consumed locally. It is therefore very advantageous to offload the cooperative perception application to the MEC servers of 5G. On one hand, as the MEC servers are much more powerful in computing than the onboard computers, the processing time needed for fusing the multi-source data can be reduced. On the other hand, as compared to cloud-computing based implementation, the delay caused by routing through the backhaul network is eliminated since the data transmission remain local. As a result, up-to-date LDMs can be provided to the users. When the percentage of automated vehicle in traffic (namely, the penetration rate) is large enough, LDMs can even be generated at a rate much higher than CSMs. More importantly, because messages are all gathered to and disseminated by the powerful local centers, security issues such as authentication, authorization and encryption can be better addressed to protect the vehicles against malicious attacks [9], [42]. In addition, by leveraging the information of the traffic environment provided by the LDMs, C-ITS applications can also be implemented at the MEC servers and provided to the traditional vehicles and other road users with communication equipments. In this sense, the MEC servers act as the C-ITS roadside units (RSUs).

The success of this locally centralized implementation strategy relies on the high performance in both the UL transmission of CSMs and the DL dissemination of LDMs. In DL, multicast and broadcast can be enhanced for the efficient dissemination of LDMs. Meanwhile, due to that the environmental information contained in the CSMs generated by the adjacent vehicles are highly redundant, higher traffic density occurs in UL, which is quite the opposite of today's cellular networks. The high traffic density requirements can be addressed by the densification of APs, and the user-centric access strategy provides means to control interference and sustain high quality connections during mobility. Yet, to serve

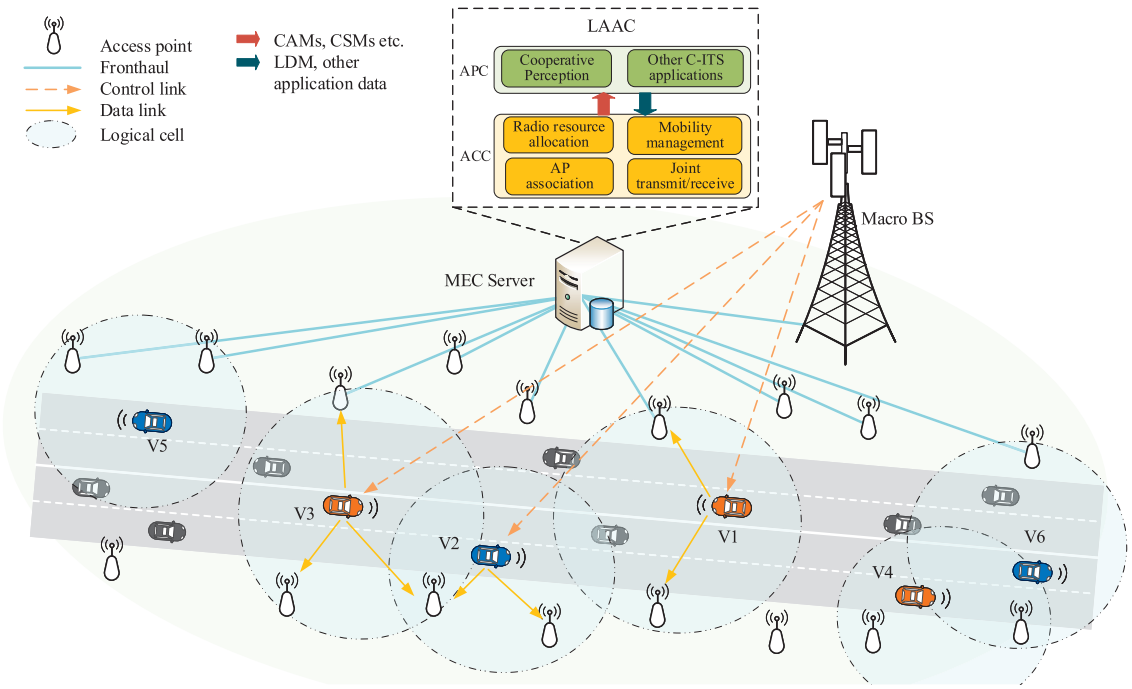

FIGURE 2. The architecture of the proposed system.

automated vehicles and reap all the promised benefits, the proactive serving AP updating and radio resource management following the users' movements are required as a precondition. The strategies proposed in existing studies on user-centric access, including those dedicated to vehicular communications [33], [37], [38], are generally channel state information (CSI) based. In vehicular networks, their implementations will cause extremely high signaling overhead considering the small coverage of the APs and the high mobility of the automated vehicles. Besides, cooperative perception as well as many other use cases feature the periodic traffic pattern, and thus semi-persistent scheduling is preferred to reduce overhead and ensure low latency [18], which also makes the CSI based strategies unsuitable.

Luckily, in UDNs the distance between a vehicle and a serving AP is short, which increases the probability line-of-sight (LOS) transmission [30], [33], especially since the lightweight APs can be deployed at strategic spots. As a consequence, the geolocation-based communication and radio resource management techniques [44]–[46] become feasible. Besides, the following particularities of vehicular communications for automated driving are observed:

- The kinematic states of the automated vehicles, i.e., their positions, velocities, accelerations, headings, etc., are what to be delivered to the application center.
- Although the vehicles are highly mobile, their movements are restricted within certain areas, e.g., on the roads and at the parking lots, and have to obey traffic laws. Thus, their future positions are largely predictable.

In other words, the kinematic information of the vehicles extracted at the application center provides good handle for mobility management of the user-centric vehicular network.

Based on the above considerations, we present a 5G-enabled user-centric system architecture for automated driving vehicles, which takes the application implementation and communication requirements into account jointly and exploits the application-layer kinematic information in user-centric access control.

B. SYSTEM DESCRIPTION

The proposed system architecture is depicted in Fig. 2 and described as follows. APs are densely deployed alongside the roads on which automated driving is permitted. Existing infrastructures, e.g. street lamps and building walls, can be exploited for their deployment. The whole area is also covered by macro base stations (BSs). Both APs and macro BSs are connected to the MEC servers by fronthaul links. The MEC servers may be deployed at the same sites with the macro BSs. Network resources sliced to vehicular communications are managed by the distributed LAACs hosted at the MEC servers.

A LAAC consists of two functional units: An APplication Center (APC), who runs the cooperative perception and other C-ITS applications, and an Access Control Center (ACC), who manages the access infrastructures and radio resources to provide communication services to the automated/cooperative vehicles in a user-centric manner. The APs, organized into logical cells, are responsible for data transmission, possibly over the frequency band dedicated

to vehicular communications, for instance the 5.9 GHz frequency band widely considered. While the control signaling is transmitted via macro BSs using a different and probably lower band.

Through the interface between ACC and APC, the facility layer messages such as CAMs and CSMs, sent by the automated/cooperative vehicles in UL, are delivered from ACC to APC, and the output LDMs by cooperative perception and other C-ITS application data are delivered in return. These data are sent in DL to the interested vehicles, using either unicast, multicast or broadcast. In the meantime, the kinematic information of all these vehicles extracted at APC and contained in the LDMs are exploited by ACC for access management.

As soon as a vehicle starts its engine, its communication terminal is turned on and a request of joining the network is sent to the control center located at the core network via macro BSs. If the request is approved, a logical cell ID is allocated to the vehicle, and the management task is handed over to the LAAC of the region where the vehicle locates. For each user, the ACC selects the serving APs of its logical cell, decides the cooperative transmit/receive strategies, allocates radio resources, and the most importantly, makes dynamic adjustments following the movement of the vehicles and the change of the network topology.

In UL, the serving APs of each vehicle perform cooperative reception of the CSMs sent over the allocated radio resources. In DL, a vehicle can still be served by its own logical cell. But a more efficient manner is to merge the logical cells of the vehicles located nearby [47] and disseminate the generated LDM using multicast/broadcast [38].

We remark here that although our initial purpose is to support cooperative perception for automated driving, it is not difficult to see that the communications requirements of many other use cases, e.g., the communications with backend servers for infotainment type applications, can also be addressed based on the established system architecture, as long as the UL/DL transmission has a role to play. Yet, the specific access strategies shall be adjusted according to the traffic pattern and communications requirements.

IV. KINEMATIC INFORMATION AIDED USER-CENTRIC ACCESS

In this section, we discuss how the kinematic information of the vehicles can be exploited in the design of the user-centric access strategies. Issues brought about by practical network deployments and constraints are also discussed. The UL transmission of the periodic CSMs is considered. We notice that most of the works in infrastructure-based vehicular communications, including those with user-centric access [37], [38], are devoted to DL. Yet to the best of our knowledge, much fewer studies are dedicated to UL.

Recall that high data rate, low E2E latency, and high reliability are required. The requirements on data rate and reliability can be transferred to the requirement on the received signal-to-interference-plus-noise ratio (SINR). E2E latency, which is the time difference between the generation of CSM at the vehicle and the successful receiving at the MEC server, is composed of the queuing delay, over-the-air transmission delay, processing delay, and retransmission delay [48]. All these terms shall be constrained to reduce the E2E latency.

A. AP ASSOCIATION AND JOINT RECEIVING

Since the positions of the APs and vehicles are available, serving APs of a logical cell can be selected using position-related strategies. For instance, a certain number of APs closest to the vehicle, or the APs within a certain distance to the vehicle, could be selected. Due to the short propagation distances between a vehicle and a serving AP, the channel condition will be good if an LOS path exist. However, severe shadow fading may occur because the LOS path could be blocked by obstacles such as buses and trees in practical scenarios. Besides, the shadow fadings of the multiple links are spatially correlated when they cut through the same obstacles [49]. Therefore, it is important to select the serving APs from different directions, rather than based on the distances solely.

The logical cells of different vehicles can overlap but will be allocated with separate time-frequency resources to avoid interference. In practice, the maximum number of users that an AP can serve could be constrained, due to the limited processing capability and fronthaul capacity. On the other hand, vehicles are distributed unevenly over the space. For instance, the vehicle density is generally higher at intersections. Therefore, the AP association strategy has to take load balancing into consideration.

The UL transmission of CSMs requires both high data rate and high reliability. If the APs only have RF unit, then all the baseband processing will be executed at the MEC server. In this case many advanced CoMP joint receiving technologies, such as the maximum ratio combining (MRC), can be applied. If the APs has baseband processing capability, then the serving AP may perform reception independently. The diversity gain achieved is lower compared to MRC, but much less burden is imposed on the fronthaul. Thus, the later strategy is more suitable if the capacity of the fronthaul is limited. The fronthaul capacity limitation is an important issue to consider, since wireless fronthauling [50] is becoming an attractive solution to UDN.

It is very likely that antenna arrays and multiple RF chains are equipped on the vehicles, thanks to their large physical sizes. Then a multiple-input multiple-output (MIMO) system can be formed and diverse MIMO technologies can be exploited. Both multiplexing gain and diversity gain can be achieved, such that data rate and reliability can be both improved. In [44], a geolocation-based beamforming technique was proposed considering the high LOS transmission probability in UDN, which may also be used by the vehicles in this case. Moreover, multi-connectivity using different time-frequency resource assignments [51] could also be allowed, which will make the access design more flexible.

B. RADIO RESOURCES ALLOCATION

The time-frequency resources are divided into orthogonal resource blocks (RBs) and shared by the vehicles. Since the transmission of CSMs is periodic, semi-persistent strategies are required to ensure low latency. Moreover, as the sizes of the CSMs generated by different vehicles are bounded, the same amount of resources can be allocated to each vehicle. For the convenience in discussion, we assume that the resources are divided such that a CSM can be delivered over one RB.

The UL transmissions from vehicles allocated with a same RB will interfere each other. Hence, an important task of the RBs allocation strategy is to perform interference control. Due to the short propagation distance, it is possible to allocate RB based on the relative positions of the vehicles. For instance, following the strategy proposed for LTE-V2V [6], an RB reuse distance can be defined, and each two vehicles located within the reuse distance are not allowed to transmit over the same RB. Clearly, the selection of the reuse distance also impacts the received SINR.

The RB allocation strategy shall take the delay constraints into consideration as well. Specifically, it determines both the queuing delay and the over-the-air transmission delay. The CSMs are generated by the onboard perception systems of the automated vehicles at a same rate, but random time instances. After a CSM is generated, it is stored in the cache waiting to be transmitted. It is expected that an RB can be allocated as soon as possible to minimize the queuing delay. However, only those RBs not occupied by the nearby vehicles can be allocated for the interference control purpose. Thus, a maximum queuing delay constraint shall apply. On the other hand, there are different ways to divide the time-frequency resources [48]: An RB can be made wider in the time domain and narrower in the frequency domain, or the opposite, yet the same amount of data can be conveyed. In the former case, more vehicles are allowed to transmit at the same time and the queuing delays can be reduced, but larger over-the-air delays will be caused. In the latter case the outcomes are reversed. Yet their impacts on the overall performance might be different, and thus a careful evaluation is needed.

If the packet reception fails, the vehicle may need to retransmit the CSM using a different RB. To ensure low latency and high reliability, a dedicated resource pool for retransmission could be reserved. However, this will diminish the overall spectrum efficiency. In this regard, the reserved RBs shall be selected after carefully assessing the impacts on the performances of the initial transmission and retransmission.

In addition to the time-frequency resources, ACCs may also need to control the transmit power of the vehicles. Considering that the APs are densely deployed and a vehicle is served by multiple APs, it is feasible to fix the transmit power of the vehicles according to the target received SINR level, as long as the topology of the APs remain unchanged. However, the density of the vehicles also varies over time. During hours when the vehicle density is low, e.g., in the nights, part of the APs can be turned into idle/sleep mode for the energy saving purpose. The topology of the network will therefore be changed, and the average transmission distance will get longer. Thus, the transmit power should be adjusted accordingly to maintain the SINR level.

C. MOBILITY SUPPORT

Since the position, heading, velocity and acceleration of the vehicles are known to the ACC, it can renew the serving APs proactively by estimating the future locations of the vehicles. Current members of the logical cells may be removed, and new APs added in. The change is transparent to the vehicle. The development of effective algorithms is required.

As the vehicles move in different speed and direction, their relative positions will change over time. Therefore, the ACC needs to track and predict the positions of the vehicles transmitting over a same RB. Once it finds that two co-channel vehicles are too close, a new RB will be reallocated to one of them. There's a tradeoff between efficiency and performance in the design of resource management algorithms. There are many factors to be considered regarding performance, such as the interference level and the sustainable duration before the next adjustment has to be made. The performance can be optimized by searching over the feasible RBs exhaustively, but the cost of high computational complexity and low time-efficiency. Or the efficiency can be improved with performance degradation.

It should be noted that the whole area will be divided into many regions and each managed by a LAAC. When the vehicles maneuver across two adjacent regions, the access management task will be handed over from the current LAAC to the one of the target regions, in a proactive manner as well. The interface between the LAACs will play a very important role in this system. Via this interface, information of the vehicles located near the borders, on both their kinematic states and access organizations, shall be exchanged frequently. These information are required not only by the handover process, but also by the distributed access management algorithms.

V. NUMERICAL BENCHMARKING

In this section, we evaluate by simulation the performance of the proposed architecture in support of the period UL transmission of CSMs in simple scenarios. The purpose is to examine if the UL traffic can be accommodated by the user-centric ultra-dense network and whether the latency and reliability requirements can be met. Therefore, strategies related to issues link serving AP updating and RB re-allocation regarding user mobility are not given, which are left for further study. Rather than trying to find the optimal ones, we employ practical access strategies in the simulation to provide benchmark to future works.

A. SCENARIO MODELS AND ACCESS STRATEGIES

An urban freeway scenario and an urban intersection scenario are considered, whose 2D models are depicted in Fig. 3. In the

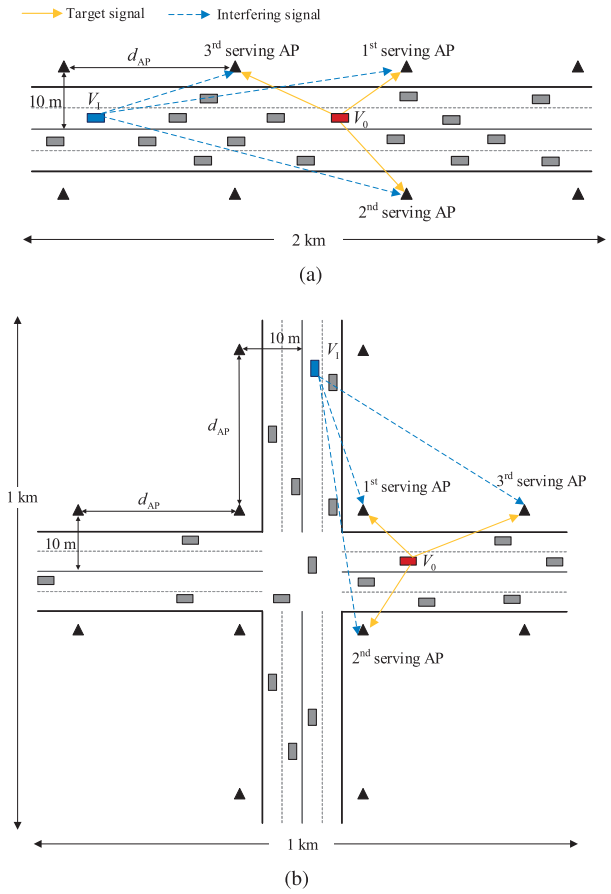

FIGURE 3. 2D models of the simulated scenarios. (a) Freeway scenario. (b) Intersection scenario.

freeway scenario, the road segment is of 2 km long, while in the intersection scenario, two perpendicular road segments, each of 1 km long, intersect at their midpoints. All roads have double 3.5 meter-wide lanes on each side. Vehicles are distributed along the central line on each lane. Their positions follow a 1D homogeneous Poisson point process (PPP). The average inter-vehicle distance is given by d_{VEH} in meters. Accordingly, the density of the vehicles on each road is given by $4000/d_{\mathrm{VEH}}$ vehicles per kilometer. APs are symmetrically and uniformly distributed along the two sides of the roads, and the distance between two neighboring APs is denoted by d_{AP} in meters. Single antenna is assumed at both APs and vehicles, and the antenna heights are denoted respectively by h_{AP} and h_{VEH} in meters. Each end of the roads is extended by 1 km in the simulation, but the vehicles located on the extended parts are not accounted in performance evaluation.

All vehicles on the freeway are assumed to be automated vehicles who generate CSMs periodically and wish to send them to the MEC server in UL. The message rate is fixed to be $f_b = 10$ Hz, and the payload size is given by 6000 bytes. The time instances when the CSMs are generated by the vehicles are randomly selected over the message period $T = 1/f_b = 100$ ms, following the uniform distribution. A dedicated bandwidth of $B = 20$ MHz at central frequency $f_c = 5.9$ GHz is allocated. Namely, there is no interference from other traffic. An RB is set to occupy the entire bandwidth in the frequency domain and 1 ms in the time domain. Thus, the $T \times B$ time-frequency resources are divided into 100 RBs in total, denoted by $\{\mathtt{RB}_1, \mathtt{RB}_2, \ldots, \mathtt{RB}_{100}\}$, to be shared by all the vehicles. An effective payload transmission rate of 48 Mbps is required to transmit a CSM of 6000 bytes over 1 ms. We set the SINR threshold τ at the receiver to be 12 dB, upon which the Shannon channel capacity over 20 MHz bandwidth is approximately 81.5 Mbps. When the received SINR reaches this threshold, the CSM is considered reliably received.

Consider an automated vehicle V_0 and denote its CSM generation moment by t_0, $t_0 \sim \mathrm{uni}(0, T]$. K serving APs are selected according to the 2D distance to V_0. Considering the symmetry in AP distribution and the possible spatial correlation in shadow fadings, the following strategy is used. The first candidate is the AP (on the same side of the road where V_0 is located) closest to V_0; the second candidate is the one on the opposite side, closest to V_0; the third candidate is the one on the same side, second closest to V_0; and so forth.

The RB allocation strategy takes both queuing delay control and interference control into account. A maximum queuing delay L in milliseconds, and an RB reuse distance D in meters are defined. It is required that an RB shall be assigned to a vehicle within L ms limit after its CSM is generated, meanwhile, an RB cannot be reused by any two vehicles whose relative distance is smaller than D m. For the sake of simplicity, the widths of the lanes are ignored, and in the intersection scenario, the distance between two vehicles is computed by the sum of their distances to the intersection point, when they locate at the two perpendicular roads respectively, as shown in Fig. 4. Specifically, the RB allocation process for V_0 is summarized as follows:

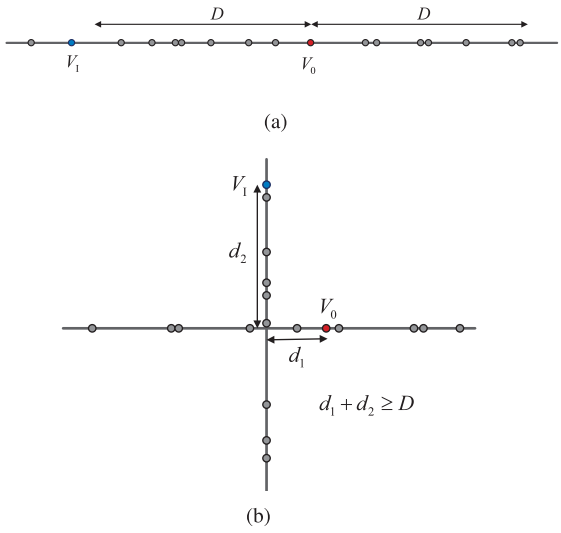

FIGURE 4. The simplified models of the simulated scenarios used for RB allocation. (a) Freeway scenario. (b) Intersection scenario.

TABLE 2. 3GPP 3D-UMi path loss model (3GPP TR36.873 [52]).

	Path loss model (f_c in GHz, distances and heights in meters)	σ_X (in dB)	Applicable range (in m)
LOS	$PL = 22\log_{10}(d_{3D}) + 28 + 20\log_{10}(f_c)$	3	$10 \le d_{2D} \le d'_{BP}$ [a]
	$PL = 40\log_{10}(d_{3D}) + 28 + 20\log_{10}(f_c) - 9\log_{10}((d'_{BP})^2 + (h_{AP} - h_{VEH})^2)$	3	$d'_{BP} \le d_{2D} \le 5000$
NLOS	$PL = \max(PL_{LOS}, PL_{NLOS})$ $PL_{NLOS} = 36.7\log_{10}(d_{3D}) + 22.7 + 26\log_{10}(f_c) - 0.3(h_{VEH} - 1.5)$	4	$10 \le d_{2D} \le 2000$

[a] d'_{BP} is the 2D breakpoint distance computed by $d'_{BP} = 4(h_{AP} - 1)(h_{VEH} - 1)f_c/c$, where $c = 3 \times 10^8$ m/s.

1: FLAG = 0, $j = \lceil t_0 \rceil$;
2: **while** $j \le \lceil t_0 \rceil + L - 1$ **do**
3: **if** $\mathtt{RB}_j$ is not used any vehicle within D m range to V_0 **then**
4: Assign $\mathtt{RB}_j$ to V_0, FLAG =1, and **break**;
5: **end if**
6: $j = j + 1$;
7: **end while**
8: **if** FLAG = 0 **then**
9: Mark V_0 as congested.
10: **end if**

If V_0 is marked congested, the CSMs it generates will not be transmitted. Otherwise, its K serving APs will attempt to receive the transmitted CSMs independently. Macro diversity gain is thus achieved. The effective received SINR is thus given by:

$$\mathtt{SINR}_{\text{eff}} = \max_{1 \le k \le K} \mathtt{SINR}_k \tag{1}$$

where $\mathtt{SINR}_k$ denotes the received SINR at the kth serving AP. If $\mathtt{SINR}_{\text{eff}}$ is below τ, then the CSM packet is considered lost. Retransmission is not allowed. Therefore, the E2E transmission delay is bounded by $L + 1$ ms.

Denoting by Ψ_{V_0} the set of vehicles that are assigned with the same RB as V_0, $\mathtt{SINR}_k$ is computed as:

$$\mathtt{SINR}_k = \frac{P_{\text{RX}}^{k,0}}{\sum_{l \in \Psi_{V_0} \setminus \{V_0\}} P_{\text{RX}}^{k,l} + N_0} \tag{2}$$

where $P_{\text{RX}}^{k,0}$ and $P_{\text{RX}}^{k,l}$ stand respectively for the target signal power from V_0 and the interfering signal power from the co-channel vehicle V_l, and N_0 is power of the additive white Gaussian noise (AWGN) with power spectrum density -174 dBm/Hz. The transmit power of each vehicle is fixed to be $P_{\text{TX}} = 10$ dBm. The received signal power is computed by (superscripts are omitted for clarity):

$$P_{\text{RX}} = P_{\text{TX}} - PL - X + \delta \quad \text{(in dBm)} \tag{3}$$

where PL, X, and δ denote the path loss, large-scale shadow fading, and small-scale multipath fading, respectively.

The employed 3D-UMi path loss model defined by 3GPP for small BS scenarios [52] is shown in Table 2, where d_{2D} and d_{3D} stand respectively for the 2D and 3D (counting heights) distance between an AP and a vehicle, and σ_X for the standard deviation of the lognormal shadow fading X. The model distinguishes LOS and non-line-of-sight (NLOS) transmission situations, and the LOS probability is given by:

$$\text{Pr}_{\text{LOS}} = \min\left(\frac{18}{d_{2D}}, 1\right) \cdot \left(1 - \exp\left(-\frac{d_{2D}}{36}\right)\right) + \exp\left(-\frac{d_{2D}}{36}\right) \tag{4}$$

According to (4), the LOS probability is 1 when $d_{2D} \le 18$ m. The multipath fading δ follows the Rayleigh distribution.

Since the performance of cooperative perception is determined by the reception reliability level of CSMs from all vehicles rather than from a single one, the performance is evaluated from the perspective of the whole system. Three performance metrics are defined:

- The Congestion Rate (CR), denoted by P_{CR}, is defined to be the ratio of congested vehicles, i.e., those without RB assigned within the queuing delay limit, in all vehicles on the road segment.
- The Packet Loss Rate (PLR), denoted by P_{PLR}, is defined to be the ratio of vehicles whose CSMs are lost, i.e., whose effective received SINRs do not reach τ, in all vehicles with RB assigned.
- The outage probability, denoted by P_{out} and computed as

$$\begin{aligned} P_{\text{out}} &= 1 - (1 - P_{\text{CR}})(1 - P_{\text{PLR}}) \\ &= P_{\text{CR}} + P_{\text{PLR}} - P_{\text{CR}}P_{\text{PLR}} \end{aligned} \tag{5}$$

stands for the probability that the CSMs generated by any vehicle in the network fail to be transferred to the MEC server within the E2E latency limit.

Clearly, it is important to lower down both CR and PLR for a high overall reliability.

B. SIMULATED RESULTS

1) IMPACTS OF *L* AND *D*

Firstly, we set $d_{\text{AP}} = 30$ m, $h_{\text{AP}} = 10$ m and $h_{\text{VEH}} = 1.5$ m in both scenarios. The RB reuse distance D are chosen from {75 m, 100 m, 125m} and the queuing delay limit L from {4 ms, 6 ms, 8 ms}. The average CRs, PLRs, and outage probabilities are plotted against the average inter-vehicle distance d_{VEH}, which varies from 10 m to 50 m, in Fig. 5, Fig. 6, and Fig. 7 respectively. Assuming the lengths of all vehicles be 5 m, the average gaps correspond to the 2-second safety distance at speed between 9 km/h and 81 km/h, and

represent scenarios from traffic jam to smooth traffic. Note that the vehicle density is inversely proportional to d_{VEH}. The results are averaged over up to 2×10^5 system realizations. In each realization, 20 CSMs are sent from each vehicle on the road segment, whose positions are not changed but an independent channel realization is generated for each CSM. In all figures in this section, the results obtained with $D = 75$ m are plotted in red, $D = 100$ m in blue, and $D = 125$ m in green.

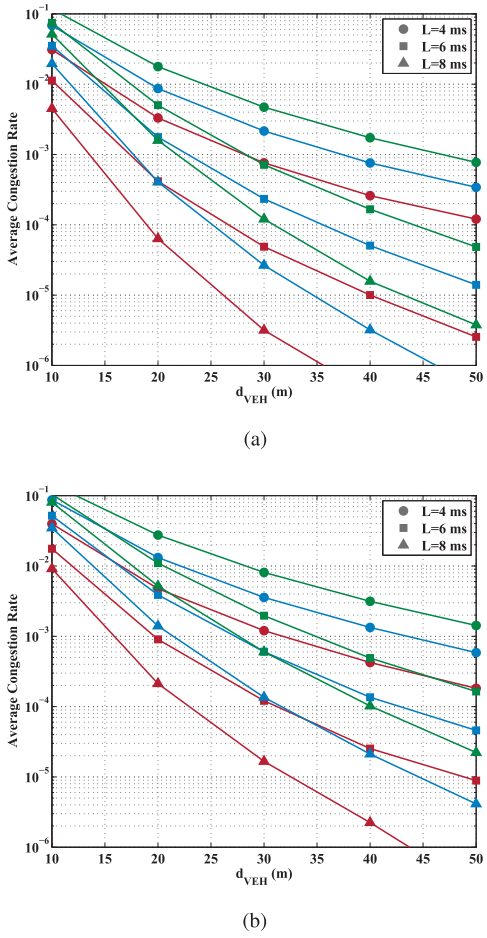

FIGURE 5. Average congestion rates in different RB reuse distance and queuing delay limit settings, when $h_{\mathrm{AP}} = 10$ m, $d_{\mathrm{AP}} = 30$ m. (a) Freeway scenario. (b) Intersection scenario.

It can be clearly seen from Fig. 5 that CR is determined by both the queuing delay limit L and the vehicle density. Both the shrinking of L and the decreasing of d_{VEH} (the growing of the vehicle density) will degrade CR. When d_{VEH} and L are fixed, CR can be reduced by selecting a smaller D. Since the number of competing vehicles is larger in the intersection scenario, higher CRs are resultant at the same d_{VEH} and L settings, as compared to the freeway scenario.

Fig. 6 shows that PLR also grows as the vehicle density increases, but at a much slower rate as compared with that of CR. The change of L has little impact on PLR, as the percentage of congested vehicles is small enough in all setups. However, PLR can be brought down by increasing D,

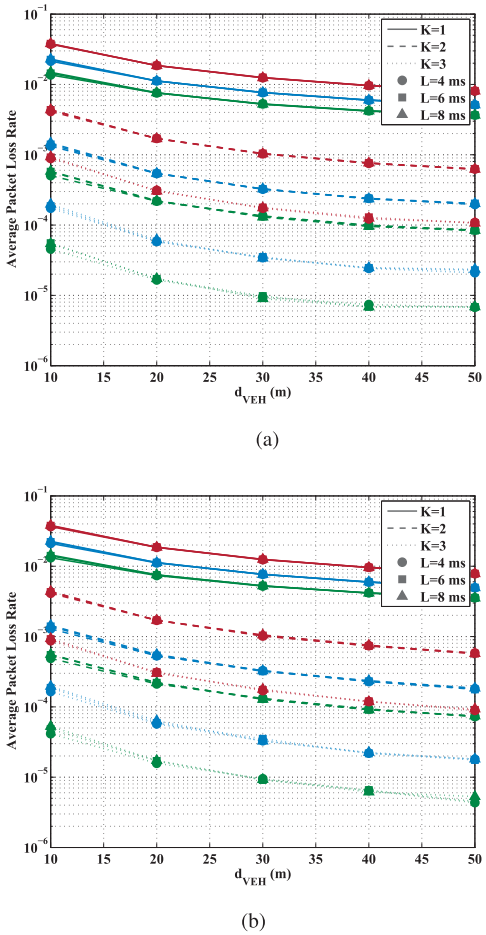

FIGURE 6. Average packet loss rates in different RB reuse distance and queuing delay limit settings, when $h_{\mathrm{AP}} = 10$ m, $d_{\mathrm{AP}} = 30$ m. (a) Freeway scenario. (b) Intersection scenario.

such that the co-channel interferers are segregated further apart, or by increasing K for higher diversity gain. The gaps between the PLRs achieved under the two different scenarios are much smaller comparing to those between CRs, because the interferers are spaced apart effectively.

Since the change in D has opposite impacts on CR and PLR, a tradeoff exists when selecting D. It can be seen from Fig. 7 that with different L, the relationships of the outage probability curves obtained with different choices of D are distinct. Therefore, D should be optimized carefully under different user densities, communication requirements, and scenarios. An outage probability of 10^{-5} is reached in the freeway scenario, when $d_{\mathrm{VEH}} = 50$ m, $L = 8$ms, $D = 125$ m and $K = 3$. However, when the vehicle density is very large ($d_{\mathrm{VEH}} = 10$ m), it is uneasy to reduce the outage probability even to below 10^{-2} owing to the large CRs. To improve the outage performance, it is possible to reduce CRs by choosing a smaller D, and then increasing K to make up for the degradation brought to PLR. However, it should be noted that the shortage in RBs is the essential constraint, and meanwhile, a larger K means higher requirements on the capacity of the fronthaul links and the processing capability of the APs.

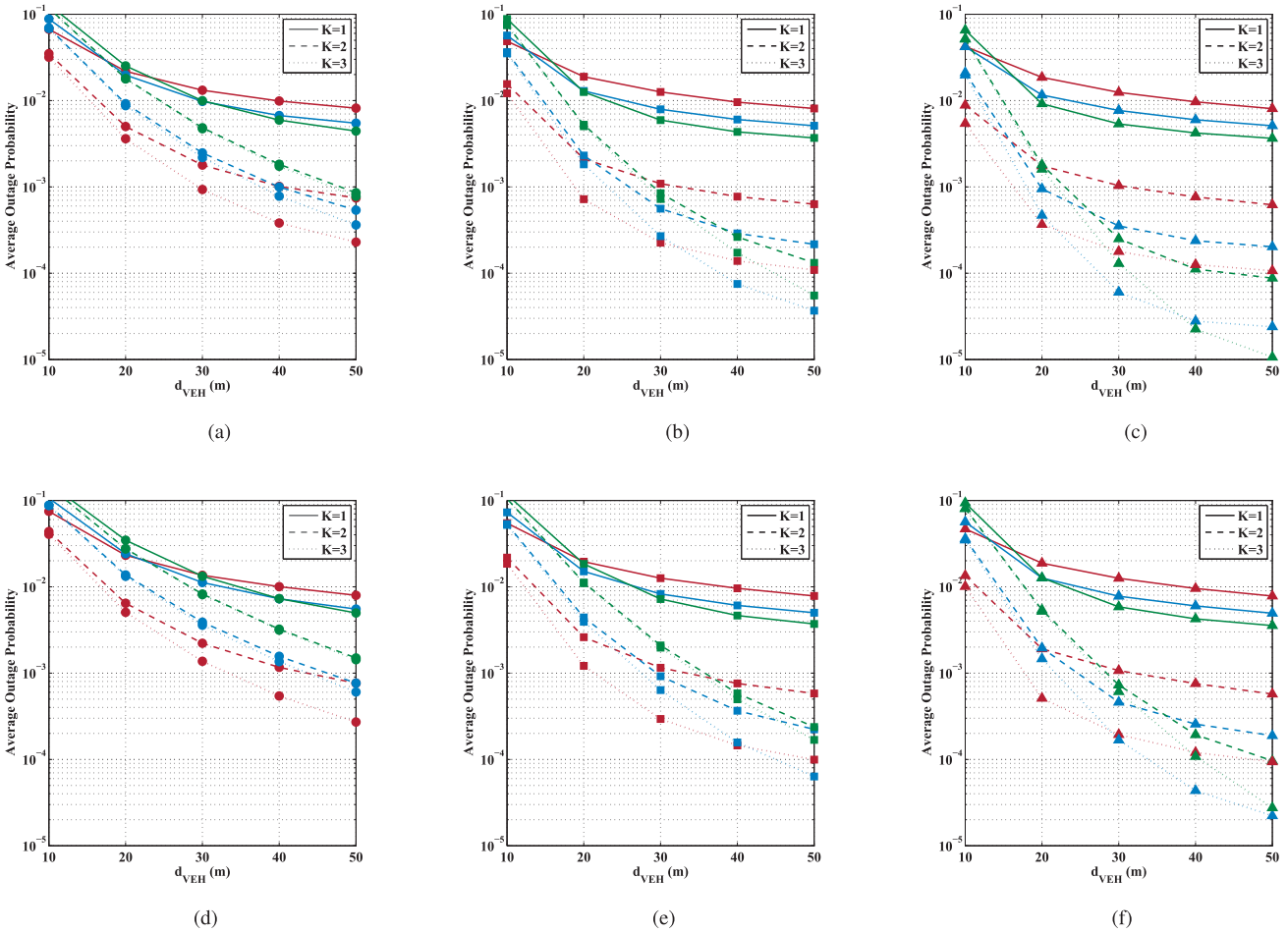

FIGURE 7. Average outage probabilities in different RB reuse distance and queuing delay limit settings, when $h_{AP} = 10$ m, $d_{AP} = 30$ m. (a) Freeway scenario, $L = 4$ ms. (b) Freeway scenario, $L = 6$ ms. (c) Freeway scenario, $L = 8$ ms. (d) Intersection scenario, $L = 4$ ms. (e) Intersection scenario, $L = 6$ ms. (f) Intersection scenario, $L = 8$ ms.

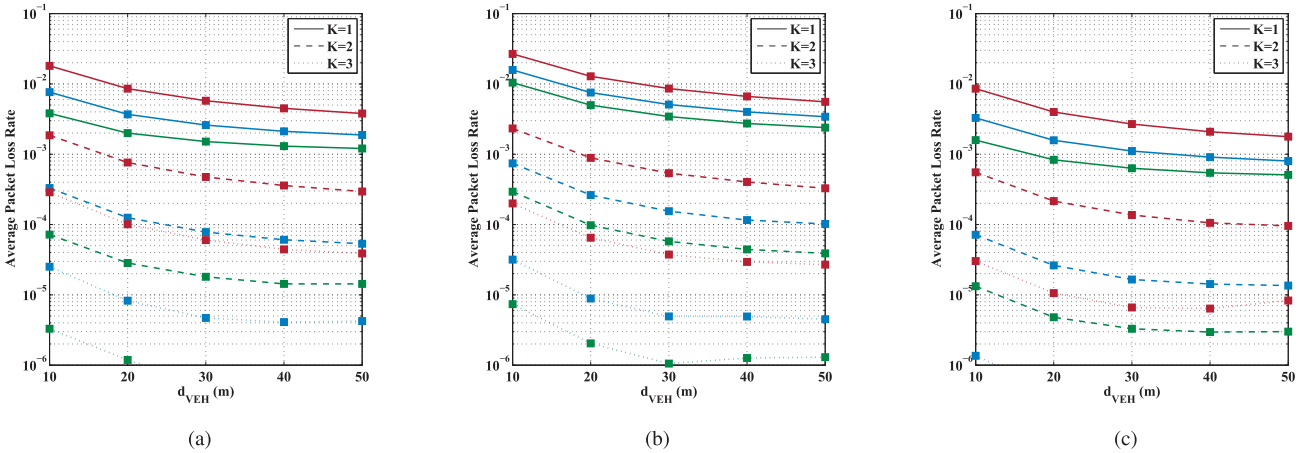

FIGURE 8. Average packet loss rates under different AP deployment configurations, with $L = 8$ ms and varying D. (a) $h_{AP} = 3$ m, $d_{AP} = 30$ m. (b) $h_{AP} = 10$ m, $d_{AP} = 10$ m. (c) $h_{AP} = 3$ m, $d_{AP} = 10$m.

2) IMPACTS OF AP DEPLOYMENTS

Next, the performances are evaluated under different AP deployments, with L fixed to be 8 ms, and D selected from {75 m, 100 m, 125m}, in the freeway scenario. Similar impacts are expected in the intersection scenario. Three setups are considered: 1) $h_{AP} = 3$ m, $d_{AP} = 30$ m, 2) $h_{AP} = 10$ m, $d_{AP} = 10$ m, and 3) $h_{AP} = 3$ m, $d_{AP} = 10$ m. Since the AP deployment has nothing to do with the employed

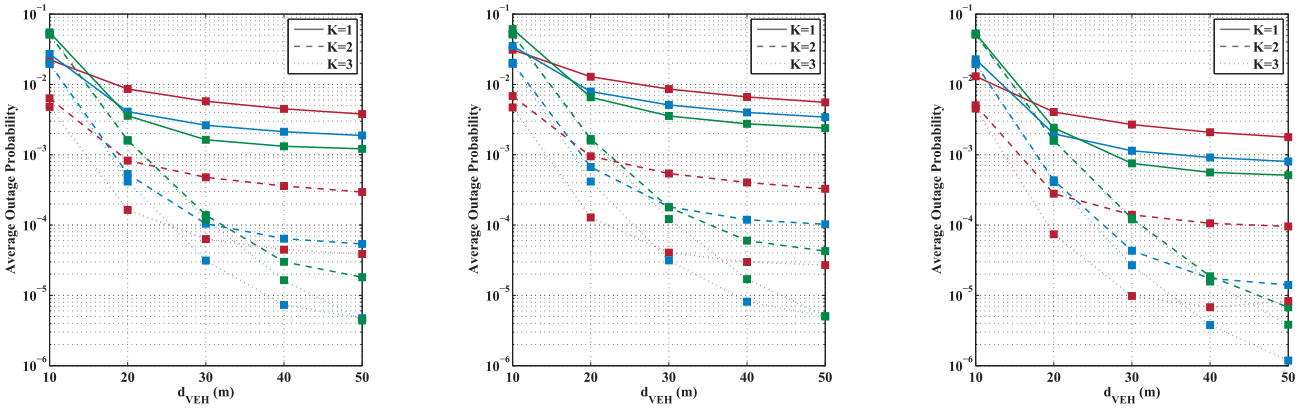

FIGURE 9. Average outage probabilities under different AP deployment configurations, with $L = 8$ ms and varying D. (a) $h_{AP} = 3$ m, $d_{AP} = 30$ m. (b) $h_{AP} = 10$ m, $d_{AP} = 10$ m. (c) $h_{AP} = 3$ m, $d_{AP} = 10$m.

TABLE 3. Statistics of $\mathtt{SINR}_{\mathrm{eff}}$.

Parameter setups (h_{AP}, d_{AP}, D, K)	3, 10, 125, 2	3, 30, 100, 3	10, 10, 100, 3	10, 30, 125, 3
$\mathrm{E}(\mathtt{SINR}_{\mathrm{eff}})$ (in dB)	47.43	45.07	45.27	42.81
$\mathrm{Var}(\mathtt{SINR}_{\mathrm{eff}})$ (in dB^2)	28.58	57.78	17.81	20.23
$\Pr(\mathtt{SINR}_{\mathrm{eff}} \leq 12\mathrm{dB})$	3.11×10^{-6}	4.95×10^{-6}	5.91×10^{-6}	7.16×10^{-6}
Average PLR (from Fig. 6(a) and Fig. 8)	2.99×10^{-6}	4.24×10^{-6}	4.50×10^{-6}	6.87×10^{-6}

RB allocation strategy, the CR performances remain the same as those shown in Fig. 5(a) (marked by triangles). The average PLRs and outage probabilities are plotted in Fig. 8 and Fig. 9, respectively.

By comparing Fig. 8 and Fig. 6, it can be clearly seen that PLRs are reduced by either decreasing h_{AP} or shrinking d_{AP}. By reducing h_{AP}, the 3D distance between a vehicle and a serving AP is shortened. Hence, the pathloss is reduced and the received SINR is improved. The shrinking of d_{AP} also helps to reduce the transmission distance and improve the channel condition. More importantly, it increases the LOS transmission probability. As a result, when d_{AP} is set to be a smaller value, the improvement in the PLR performance brought about by reducing h_{AP} is significantly greater for any K. Eventually, comparing Fig. 9 with Fig. 7, it can be seen the 10^{-5} outage probability target is achieved in more setups.

To provide more detailed information on the reliability performance, in Fig. 10 the cumulative distribution functions (CDFs) of $\mathtt{SINR}_{\mathrm{eff}}$ obtained in all system realizations under the freeway scenario, are plotted for $L = 8$ ms and $d_{\mathrm{VEH}} = 50$ m with different system setups. The effective received SINR is studied because the link-level transmission reliability is often more interested. Some important statistics are given in Table 3. For most transmissions, the achieved effective SINRs are high enough. When we look at the tail distribution, it can be seen that the probabilities of $\mathtt{SINR}_{\mathrm{eff}} \leq 12$ dB are constrained to below 10^{-5} in all setups, with actual values quite approximate to the average PLRs. This is

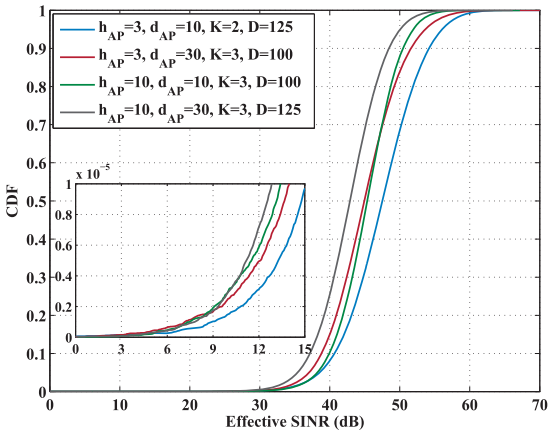

FIGURE 10. CDFs of the effective SINR under the freeway scenario with different system setups, when $L = 8$ ms and $d_{\mathrm{VEH}} = 50$ m.

understandable because if the PLR in one system realization is large, the average PLR will be pulled up considerably. It is also interesting to note that when (h_{AP}, d_{AP}, D, K) are given by (3, 10, 125, 2), the mean of $\mathtt{SINR}_{\mathrm{eff}}$ is the highest among all but the variance is also the largest. This is because a larger K ($K = 3$ in all the other three setups) can effectively help reducing the variance due to the diversity gain.

Still, it has to be emphasized that the performance metrics employed here may not be the most suitable to the cooperative perception application. When the vehicle density increases, the amount of CSMs generated per unit area and time also

becomes larger, since the message rate is set fixed, yet the information contained in the CSMs becomes more redundant. Besides, a large vehicle density usually means that the average speed is low, namely, the environment is less dynamic. Therefore, it is feasible to reduce the message rate without degrading the performance of cooperative perception. In ETSI ITS-G5 this is addressed by the Decentralized Congestion Control (DCC) function. Also, it is critical to define performance metrics better suit the application and much more work is needed in the future.

VI. CONCLUDING REMARKS

In this paper, a kinematic information aided user-centric ultra-dense vehicular network architecture has been proposed to support cooperative perception for automated driving, by carefully considering the application and the technology directions of 5G jointly. In particular, the network features distributed LAACs hosted at the MEC servers, acting both as application centers and user-centric access control centers. Focused on the UL transmission of the periodic CSMs, the possible designs of kinematic information aided user-centric access strategies, covering AP association, joint receiving, radio resources allocation, and mobility support, have been discussed. A practical benchmarking strategy set has also been proposed and evaluated by computer simulation under simple scenarios. The results have shown that the requirements on supportable vehicle density, data rate, reliability, and latency could be met at the same time, but with careful selection of the key parameters.

However, a lot more works are required even just regarding the proposed benchmarking strategy set. The parameters of the AP association strategy and RB allocation strategy should be optimized under different system deployments and practical constraints. Towards that, the analytical evaluations of the performance metrics would be necessary. Following the discussions in Section IV, practical algorithms need to be developed and their performances to be evaluated in different scenarios, with realistic assumptions and constraints, and considering practical time- and space-varying distributions of the vehicles. Especially, mobility models of the vehicles shall be included, and algorithms for dynamic space-time-frequency resource management following the vehicles' movements are desired. As mentioned at the end of the previous section, it is also important to define performance metrics that are better suit the application need. Finally, it is vital to study the impacts of the errors in the kinematic states on the system performances.

ACKNOWLEDGMENT

The authors would like to thank the Key Laboratory of Network Oriented Intelligent Computation.

REFERENCES

[1] Z. MacHardy, A. Khan, K. Obana, and S. Iwashina, "V2X access technologies: Regulation, research, and remaining challenges," *IEEE Commun. Surveys Tuts.*, vol. 20, no. 3, pp. 1858–1877, 3rd Quart., 2018.

[2] T. Luettel, M. Himmelsbach, and H.-J. Wuensche, "Autonomous ground vehicles—Concepts and a path to the future," *Proc. IEEE*, vol. 100, no. Special Centennial Issue, pp. 1831–1839, May 2012.

[3] S. E. Shladover, "Connected and automated vehicle systems: Introduction and overview," *J. Intell. Transp. Syst.*, vol. 22, no. 3, pp. 190–200, 2018.

[4] C. Campolo, A. Molinaro, and R. Scopigno, "From today's VANETs to tomorrow's planning and the bets for the day after," *Veh. Commun.*, vol. 2, no. 3, pp. 158–171, 2015.

[5] *Study on LTE-Based V2X Services (Release 14)*, document TR36.885, 3rd Generation Partnership Project, version 14.0.0, Jun. 2016.

[6] A. Bazzi, B. M. Masini, A. Zanella, and I. Thibault, "On the performance of IEEE 802.11p and LTE-V2V for the cooperative awareness of connected vehicles," *IEEE Trans. Veh. Technol.*, vol. 66, no. 11, pp. 10419–10432, Nov. 2017.

[7] R. Hult, G. R. Campos, E. Steinmetz, L. Hammarstrand, P. Falcone, and H. Wymeersch, "Coordination of cooperative autonomous vehicles: Toward safer and more efficient road transportation," *IEEE Signal Process. Mag.*, vol. 33, no. 6, pp. 74–84, Nov. 2016.

[8] L. Hobert, A. Festag, I. Llatser, L. Altomare, F. Visintainer, and A. Kovacs, "Enhancements of V2X communication in support of cooperative autonomous driving," *IEEE Commun. Mag.*, vol. 53, no. 12, pp. 64–70, Dec. 2015.

[9] J. Petit and S. E. Shladover, "Potential cyberattacks on automated vehicles," *IEEE Trans. Intell. Transp. Syst.*, vol. 16, no. 2, pp. 546–556, Apr. 2015.

[10] 5G-PPP. (2015). *5G Automotive Vision*. [Online]. Available: https://5g-ppp.eu/white-papers/

[11] A. Rauch, F. Klanner, R. Rasshofer, and K. Dietmayer, "Car2X-based perception in a high-level fusion architecture for cooperative perception systems," in *Proc. IEEE IV*, Jun. 2012, pp. 270–275.

[12] S.-W. Kim *et al.*, "Multivehicle cooperative driving using cooperative perception: Design and experimental validation," *IEEE Trans. Intell. Transp. Syst.*, vol. 16, no. 2, pp. 663–680, Apr. 2015.

[13] S.-W. Kim, W. Liu, M. H. Ang, E. Frazzoli, and D. Rus, "The impact of cooperative perception on decision making and planning of autonomous vehicles," *IEEE Intell. Transp. Syst. Mag.*, vol. 7, no. 3, pp. 39–50, Jul. 2015.

[14] J. Á. L. Calvo and R. Mathar, "A multi-level cooperative perception scheme for autonomous vehicles," in *Proc. IEEE ITST*, May 2017, pp. 1–5.

[15] *Perspectives on Vertical Industries and Implications for 5G*, NGMN Alliance, Frankfurt, Germany, 2016.

[16] *Study on Enhancement of 3GPP Support for 5G V2X Services (Release 15)*, document TR22.886, 3rd Generation Partnership Project, Version 15.1.0, Mar. 2017.

[17] M. Boban, A. Kousaridas, K. Manolakis, J. Eichinger, and W. Xu, "Connected roads of the future: Use cases, requirements, and design considerations for vehicle-to-everything communications," *IEEE Veh. Technol. Mag.*, vol. 13, no. 3, pp. 110–123, Sep. 2018.

[18] C. Campolo, A. Molinaro, A. Iera, and F. Menichella, "5G network slicing for vehicle-to-everything services," *IEEE Wireless Commun.*, vol. 24, no. 6, pp. 38–45, Dec. 2017.

[19] M. Lauridsen, L. C. Gimenez, I. Rodriguez, T. B. Sorensen, and P. Mogensen, "From LTE to 5G for connected mobility," *IEEE Commun. Mag.*, vol. 55, no. 3, pp. 156–162, Mar. 2017.

[20] G. Pocovi, H. Shariatmadari, G. Berardinelli, K. Pedersen, J. Steiner, and Z. Li, "Achieving ultra-reliable low-latency communications: Challenges and envisioned system enhancements," *IEEE Netw.*, vol. 32, no. 2, pp. 8–15, Mar./Apr. 2018.

[21] P. Popovski *et al.*, "Wireless access for ultra-reliable low-latency communication: principles and building blocks," *IEEE Netw.*, vol. 32, no. 2, pp. 16–23, Mar./Apr. 2018.

[22] A. Gupta and E. R. K. Jha, "A survey of 5G network: Architecture and emerging technologies," *IEEE Access*, vol. 3, pp. 1206–1232, Jul. 2015.

[23] Y. C. Hu, M. Patel, D. Sabella, N. Sprecher, and V. Young, "Mobile edge computing—A key technology towards 5G," ETSI, Sophia Antipolis, France, White Paper 11, Sep. 2015.

[24] S. Wang, X. Zhang, Y. Zhang, L. Wang, J. Yang, and W. Wang, "A survey on mobile edge networks: Convergence of computing, caching and communications," *IEEE Access*, vol. 5, pp. 6757–6779, 2017.

[25] S. Andreev *et al.*, "Exploring synergy between communications, caching, and computing in 5G-grade deployments," *IEEE Commun. Mag.*, vol. 54, no. 8, pp. 60–69, Aug. 2016.

[26] J. Liu, J. Wan, B. Zeng, Q. Wang, H. Song, and M. Qiu, "A scalable and quick-response software defined vehicular network assisted by mobile edge computing," *IEEE Commun. Mag.*, vol. 55, no. 7, pp. 94–100, Jul. 2017.
[27] X. Huang, R. Yu, J. Kang, Y. He, and Y. Zhang, "Exploring mobile edge computing for 5G-enabled software defined vehicular networks," *IEEE Wireless Commun.*, vol. 24, no. 6, pp. 55–63, Dec. 2017.
[28] Z. Ning, P. Dong, X. Kong, and F. Xia, "A cooperative partial computation offloading scheme for mobile edge computing enabled Internet of Things," *IEEE Internet Things J.*, to be published.
[29] Z. Ning, J. Huang, and X. Wang, "Vehicular fog computing: enabling real-time traffic management for smart cities," *IEEE Wireless Commun.*, vol. 26, no. 1, pp. 87–93, Feb. 2019.
[30] M. Kamel, W. Hamouda, and A. Youssef, "Ultra-dense networks: A survey," *IEEE Commun. Surveys Tuts.*, vol. 18, no. 4, pp. 2522–2545, 4th Quart., 2016.
[31] K. Zarifi, H. Baligh, J. Ma, M. Salem, and A. Maaref, "Radio access virtualization: Cell follows user," in *Proc. IEEE PIMRC*, Sep. 2014, pp. 1381–1385.
[32] C. Liang and F. R. Yu, "Wireless network virtualization: A survey, some research issues and challenges," *IEEE Commun. Surveys Tuts.*, vol. 17, no. 1, pp. 358–380, 1st Quart., 2015.
[33] P. Kela, J. Turkka, and M. Costa, "Borderless mobility in 5G outdoor ultra-dense networks," *IEEE Access*, vol. 3, pp. 1462–1476, 2015.
[34] S. Chen, F. Qin, B. Hu, X. Li, and Z. Chen, "User-centric ultra-dense networks for 5G: Challenges, methodologies, and directions," *IEEE Wireless Commun.*, vol. 23, no. 2, pp. 78–85, Apr. 2016.
[35] C. Pan, M. Elkashlan, J. Wang, J. Yuan, and L. Hanzo, "User-centric C-RAN architecture for ultra-dense 5G networks: Challenges and methodologies," *IEEE Commun. Mag.*, vol. 56, no. 6, pp. 14–20, Jun. 2018.
[36] P. Wu, L. Ding, Y. Wang, and Y. Xiong, "Throughput analysis of vehicle-centric cooperative transmission in ultra-dense V2I networks," in *Proc. IEEE ITSC*, Nov. 2018, pp. 3749–3754.
[37] X. Ge, H. Chen, G. Mao, Y. Yang, and S. Tu, "Vehicular communications for 5G cooperative small-cell networks," *IEEE Trans. Veh. Technol.*, vol. 65, no. 10, pp. 7882–7894, Oct. 2016.
[38] T. Sahin, M. Klugel, C. Zhou, and W. Kellerer, "Virtual cells for 5G V2X communications," *IEEE Commun. Standards Mag.*, vol. 2, no. 1, pp. 22–28, Mar. 2018.
[39] *Study on Scenarios and Requirements for Next Generation Access Technologies*, document TR38.913, 3rd Generation Partnership Project, Version 15.0.0, Jun. 2018.
[40] H. Peng, L. Liang, X. Shen, and G. Y. Li, "Vehicular communications: A network layer perspective," *IEEE Trans. Veh. Technol.*, vol. 68, no. 2, pp. 1064–1078, Feb. 2019.
[41] J. Choi, V. Va, N. G.-Prelcic, R. Daniels, C. R. Bhat, and R. W. Heath, "Millimeter-wave vehicular communication to support massive automotive sensing," *IEEE Commun. Mag.*, vol. 54, no. 12, pp. 160–167, Dec. 2016.
[42] X. Wang *et al.*, "Privacy-preserving content dissemination for vehicular social networks: Challenges and solutions," *IEEE Commun. Surveys Tuts.*, to be published.
[43] B. Di, L. Song, Y. Li, and Z. Han, "V2X meets NOMA: Non-orthogonal multiple access for 5G-enabled vehicular networks," *IEEE Wireless Commun.*, vol. 24, no. 6, pp. 14–21, Dec. 2017.
[44] P. Kela *et al.*, "Location based beamforming in 5G ultra-dense networks," in *Proc. IEEE VTC-Fall*, Sep. 2016, pp. 1–7.
[45] M. Koivisto, A. Hakkarainen, M. Costa, P. Kela, K. Leppanen, and M. Valkama, "High-efficiency device positioning and location-aware communications in dense 5G networks," *IEEE Commun. Mag.*, vol. 55, no. 8, pp. 188–195, Jul. 2017.
[46] F. J. Martín-Vega, B. Soret, M. C. Aguayo-Torres, I. Z. Kovács, and G. Gómez, "Geolocation-based access for vehicular communications: Analysis and optimization via stochastic geometry," *IEEE Trans. Veh. Technol.*, vol. 67, no. 4, pp. 3069–3084, Apr. 2018.
[47] C. Xiao *et al.*, "Downlink transmission scheme based on virtual cell merging in ultra dense networks," in *Proc. IEEE VTC-Fall*, Sep. 2016, pp. 1–5.
[48] M. Bennis, M. Debbah, and H. V. Poor, "Ultra-reliable and low-latency wireless communication: Tail, risk and scale," *Proc. IEEE*, vol. 106, no. 10, pp. 1834–1853, Oct. 2018.
[49] P. Agrawal and N. Patwari, "Correlated link shadow fading in multi-hop wireless networks," *IEEE Trans. Wireless Commun.*, vol. 8, no. 8, pp. 4024–4036, Aug. 2009.
[50] U. Siddique, H. Tabassum, E. Hossain, and D. I. Kim, "Wireless backhauling of 5G small cells: Challenges and solution approaches," *IEEE Wireless Commun.*, vol. 22, no. 5, pp. 22–31, Oct. 2015.
[51] M. Kamel, W. Hamouda, and A. Youssef, "Performance analysis of multiple association in ultra-dense networks," *IEEE Trans. Commun.*, vol. 65, no. 9, pp. 3818–3831, Sep. 2017.
[52] *Study on 3D Channel Model for LTE*, document TR36.873, 3rd Generation Partnership Project, Version 12.7.0, Dec. 2017.

LIQIN DING (M'17) received the B.E., M.E., and Ph.D. degrees in information and communication engineering from the Harbin Institute of Technology, Harbin, China, in 2009, 2011, and 2017, respectively. She was with the Department of Electronics and Telecommunications, Norwegian University of Science and Technology, from 2012 to 2014, and the Department of Electronic and Electrical Engineering, The University of Sheffield, U.K., in 2016. She is currently a Postdoctoral Fellow with the School of Electronic and Information Engineering, Harbin Institute of Technology, Shenzhen, China. Her research interests include cellular-based vehicle-to-everything communication, ultra-dense networks, lattice based MIMO detection, and cooperative communications.

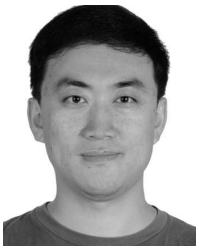

YANG WANG received the Ph.D. degree in communication and information system from the Harbin Institute of Technology, Harbin, China, in 2005. From 2005 to 2007, he was a Postdoctoral Fellow with the Shenzhen Graduate School, Harbin Institute of Technology. He has been with the School of Electronic and Information Engineering, Harbin Institute of Technology, Shenzhen, China, as an Associate Professor, since 2007. He is also a Senior Member of the Chinese Institute of Electronics. His research interests include wireless communications and signal processing, including vehicular communications, MIMO systems, MIMO channel measurement and modeling, cooperative communications, and underwater wireless charging and communication systems.

PENG WU (S'16) received the B.E. degree in information engineering from the Wuhan University of Technology, Wuhan, China, in 2015. He is currently pursuing the Ph.D. degree with the School of Electronic and Information Engineering, Harbin Institute of Technology, Shenzhen, China. He was with the Department of Science and Technology, Linkoping University, Sweden, in 2016, and the Department of Electronic and Electrical Engineering, The University of Sheffield, U.K., in 2018. His research interests include vehicular communication networks and intelligent transportation systems.

LIMING LI received the B.E. degree in communication engineering from Shandong University, Jinan, China, in 2007, and the M.S. degree in biomedical engineering from Chongqing University, Chongqing, China, in 2013. He is currently pursuing the Ph.D. degree in information and communication engineering with the Harbin Institute of Technology, Shenzhen, China. His research interests include multicarrier modulation, synchronization, equalization, and digital signal processing.

JILIANG ZHANG (M'15–SM'19) received the B.E., M.E., and Ph.D. degrees from the Harbin Institute of Technology, Harbin, China, in 2007, 2009, and 2014, respectively. He was a Postdoctoral Fellow with the Shenzhen Graduate School, Harbin Institute of Technology, from 2014 to 2016, an Associate Professor with the School of Information Science and Engineering, Lanzhou University, in 2017, and a Researcher with the Department of Electrical Engineering, Chalmers University of Technology, Gothenburg, Sweden. He is currently a Marie Curie Research Fellow with the Department of Electronic and Electrical Engineering, The University of Sheffield, Sheffield, U.K. His research interest includes wireless systems, in particular including MIMO channel measurement and modeling, single radio frequency MIMO systems, relay systems, and wireless ranging systems.